Available online at www.sciencedirect.com
SCIENCE DIRECT®

Journal of Power Sources 137 (2004) 196–205

JOURNAL OF POWER SOURCES

www.elsevier.com/locate/jpowsour

Wide range load controllable MCFC cycle with pressure swing operation

Fumihiko Yoshiba*, Yoshiyuki Izaki, Takao Watanabe

Yokosuka Research Laboratory, Chemical Energy Engineering Department, Central Research Institute of Electric Power Industry, 2-6-1 Nagasaka, Yokosuka 240-0196, Japan

Received 15 October 2003; received in revised form 19 May 2004; accepted 4 June 2004
Available online4 August 2004

Abstract

Partial load efficiencies of a natural gas fuelled MCFC/GT system are calculated; the efficiencies of four systems are compared. A constant pressure air compressor is applied in system cases 1 and 2, whereas a pressure swing air compressor is provided in system cases 3 and 4. A gas cooler is integrated in the cathode gas recycling line of cases 2–4, and an anode recycling with sub-reformer is provided in case 4. The cathode pressure loss in the MCFC stack is kept below 3 kPa during the calculation procedure to avoid a leakage of cathode gas. The range of the power load is limited to 50–100% in the constant operating pressure system (cases 1 and 2), mainly because of the limited cathode gas pressure loss of 3 kPa. The range of the power load is enlarged to 20–100% in cases 3 and 4 by combining the pressure swing operation with gas cooling in the cathode recycling line. In system cases 3 and 4, the efficiency at the lowest load operation (approx. 20–30% load) remains over 35% HHV-CH_4, whereas the maximum efficiency is calculated to be 53% HHV-CH_4 in middle load operation; the efficiency of case 4 at 100% load is estimated to be 50% HHV-CH_4. The combination of the pressure swing operation and gas cooling in the cathode recycling line offers a high efficiency of the MCFC system in a wide range of loads.

Keywords: Molten carbonate fuel cell (MCFC); Partial load thermal efficiency; Pressure swing operation; Cathode gas cooling

1. Introduction

In order to introduce molten carbonate fuel cell (MCFC) systems to distributed power, a highly efficient operation of the plant at partial load is necessary. Since the MCFC voltage under low current density conditions is quite high [1], the energy conversion efficiency of the MCFC itself is also high. However, in the case where the MCFC is combined with a gas turbine (MCFC/GT system), the efficiency of the system at partial load operation is low; the material and heat flow of the MCFC and GT is unbalanced.

Material and heat balance of the MCFC/GT and solid oxide fuel cell/gas turbine (SOFC/GT) systems were studied by some researchers [2–5]; these analyses are based on the designed (maximum power output) system conditions. Campanari [6] and Costamagna et al. [7] established a good thermal efficiency under partial load conditions in the SOFC/GT system by applying a corrected flow rate of the air compressor; a maximum thermal efficiency of the system is achieved at a power ratio of 60–100% of the designed (maximum output) power. Kimijima et al. [8] evaluated the thermal efficiency of a solid oxide fuel cell/micro-gas turbine (SOFC/GT) hybrid system at partial load operation by changing the rotation speed of the micro gas turbine; the variable speed operation of the micro gas turbine promises a superior efficiency of over 60% at a power output range of 50–100%.

The calculation of the material and heat balance in the MCFC/GT systems, on the other hand, shows that the maximum pressure loss of cathode gas should be kept lower than 3 kPa to avoid a gas leakage in the stack; hence the cathode gas is sealed by the wetability of the carbonate melt (liquid states). The cathode gas in the SOFC stack is sealed by a solid material, thus the pressure loss of the gas channel is a minor factor for stable operation. This paper presents a high efficiency MCFC/GT system operated in partial load conditions, which is achieved by applying a pressure swing air-compressor (variable rotation air-compressor) and gas cooling in the cathode gas recycling line. The main object of the calculation is to take account of the cathode gas pressure loss in the MCFC stack, which should remain lower than 3 kPa during stack operation.

* Corresponding author. Tel.: +81-46-856-2121; fax: +81-46-856-3346.
E-mail address: yoshiba@criepi.denken.or.jp (F. Yoshiba).

0378-7753/$ – see front matter © 2004 Elsevier B.V. All rights reserved.
doi:10.1016/j.jpowsour.2004.06.001

Nomenclature

A_a	frequency factor of anode resistance
$A_{c_1}, A_{c_2}, A_{c_3}$	frequency factor of cathode resistance
A_{ir}	frequency factor of internal resistance
E	Nernst voltage
E^0	standard electro-motive force
F	Faraday's constant
ΔH_a	activation energy of anode resistance
$\Delta H_{c_1}, \Delta H_{c_2}, \Delta H_{c_3}$	activation energy of cathode resistance
ΔH_{ir}	activation energy of internal resistance
j	current density
m_i	molar fraction of species i
p_i	partial pressure of species i
R	universal gas constant
R_a	anode polarisation
R_c	cathode polarisation
R_{ir}	internal resistance
T	temperature
V	cell voltage

Subscripts

a	anode
c	cathode

2. System configuration and calculating conditions

2.1. System configuration

The configuration of a reference MCFC/GT system fuelled by natural gas is illustrated in Fig. 1 [9,10]. Fuel gas is fed into the fuel reformer as steam, which leads to the CH_4 reforming and water gas shift reaction of Eqs. (1) and (2). Reformed fuel gas is supplied to the anode gas channel of the MCFC stack, and about 80% of the introduced fuel reacts according to the anode reaction of Eq. (3). Exhausted anode gas is conducted to the reformer together with the exhausted cathode gas where it is combusted to compensate for the endothermic CH_4 reforming reaction referred to in Eq. (1). The combusted gas flows into the cathode gas channel with compressed air and leads to the cathode reaction expressed in Eq. (4). Part of the exhausted cathode gas is recycled to the cathode inlet to control the temperature of the MCFC stack; the other part of the gas finds its way to the combustor, which is combined with a reformer. After all the reactions have taken place, all gases, which were fed into the MCFC, finally find their way to the expander. The total chemical reaction is similar to the combustion of fuel gas as expressed in Eq. (5); however, the main reaction of the MCFC system is based on an electrochemical reaction

CH_4 reforming reaction :

$$CH_4 + H_2O \rightarrow CO + 3H_2 \text{ (endothermic reaction)} \quad (1)$$

$$\text{water–gas shift reaction}: \quad CO + H_2O \rightarrow CO_2 + H_2 \quad (2)$$

$$\text{anode reaction}: \quad H_2 + CO_3{}^{2-} \rightarrow CO_2 + H_2O + 2e^- \quad (3)$$

$$\text{cathode reaction}: \quad CO_2 + \tfrac{1}{2}O_2 + 2e^- \rightarrow CO_3{}^{2-} \quad (4)$$

$$\text{total reaction}: \quad CH_4 + 2O_2 \rightarrow CO_2 + 2H_2O \quad (5)$$

The operating pressure and temperature of the MCFC stack is around 1 MPa and 600–660 °C, respectively. If the system is operated at partial load, the heat production in the MCFC decreases because the operating current density is reduced. The constant rotation velocity of the compressor/expander (gas turbine) is responsible for the airflow rate of the cathode gas being too high to maintain the temperature of the MCFC stack. In the reference MCFC/GT system, the sub-combustor is fitted between the air compressor and the expander, and the residual airflow from the air compressor bypasses the MCFC and is combusted in the sub-combustor together with the additional fuel supply [9,10]. The additional fuel supply is responsible for an increase in the gas turbine power when operated at partial load. Increasing the gas turbine power obstructs high efficiency of the total MCFC/GT system because although the thermal efficiency of the MCFC is high; the thermal efficiency of the gas turbine is low (turbine inlet temperature is 650–900 °C).

2.2. MCFC stack performance

A lot of power generation tests using practical sized MCFC stacks were carried out at the Central Research Institute of Electric Power Industry, CRIEPI. Prior to the stack operating tests, a 100 cm^2 bench scale single cell with the same reactive components as the stack was used for experiments. In the cell test, the gas composition of the supplied gas, the operating pressure and the operating temperature were changed; the current–voltage relation was derived according to the functions of the reactive gas partial pressure, the molar fraction of gases and the cell temperature [11].

The relation between cell voltage and current density is written as follows:

$$V \cong E - (R_{ir} + R_a + R_c)j \quad (6)$$

V and E are cell voltage and Nernst voltage, respectively, R_{ir}, R_a, R_c represent the cell resistance, and j refers to the current density. The Nernst voltage and the cell resistance are regulated as follows:

$$E = E^0 + \frac{RT}{2F} \ln \frac{p_{H_2,a} p_{CO_2,c} p_{O_2,c}^{1/2}}{p_{CO_2,a} p_{H_2O}} \quad (7)$$

Here, E^0, R, T, F, p_i describe the standard electro-motive force, universal gas constant, cell temperature, Faraday's constant and partial pressure of the gas composition i (subscripts 'a' and 'c' refer to anode and cathode), respectively. The internal resistance and the anode and cathode reaction

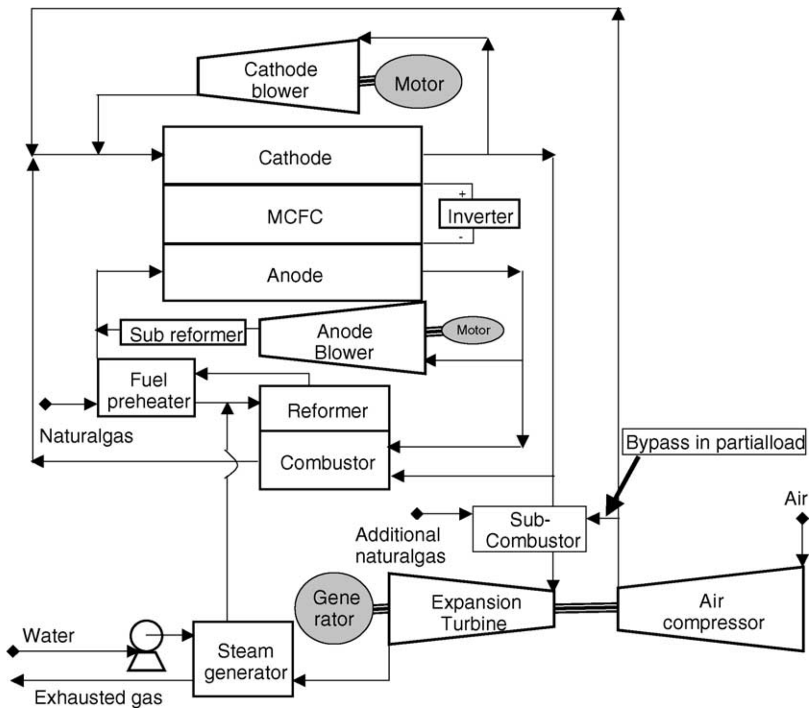

Fig. 1. Schematic pipeline of the reference MCFC/GT combined system fuelled by natural gas [9,10].

resistance are expressed as follows:

$$R_{ir} = A_{ir} \exp\left(-\frac{\Delta H_{ir}}{RT}\right) \tag{8}$$

$$R_{a} = A_{a} T \exp\left(-\frac{\Delta H_{a}}{RT}\right) P_{H_2,a}^{-0.5} \tag{9}$$

$$R_{c} = A_{c_1} T \exp\left(-\frac{\Delta H_{c_1}}{RT}\right) P_{O_2,c}^{-0.75} P_{CO_2,c}^{0.5} + A_{c_2} T \exp\left(\frac{\Delta H_{c_2}}{RT}\right) \times \left\{m_{CO_2,c} + A_{c_3} m_{H_2O,c} \exp\left(\frac{\Delta H_{c_3}}{RT}\right)\right\}^{-1} \tag{10}$$

m_i designates the mole fraction of the chemical species i, A_{ir}, A_a, A_{c_1}, A_{c_2}, A_{c_3} refer to the frequency coefficient of the internal resistance and the anode and cathode reaction resistance, ΔH_{ir}, ΔH_a, ΔH_{c_1}, ΔH_{c_2}, ΔH_{c_3} give an indication of the activation energy, respectively. Every parameter appearing in these equations is listed in Table 1. By dividing the MCFC stack into control volumes and applying the cell performance Eqs. (6)–(10) to these volumes, the electrical output power and the current density distribution in the stack can be calculated.

2.3. MCFC operating conditions required for stable power generation

In Table 2, the gas conditions required for a stable MCFC stack operation are presented. In a MCFC/GT power plant, the stack is located in a pressure vessel and the pressure vessel is filled with air, cathode gas or nitrogen; the pressure distribution surrounding the stack is constant. The cathode gas pressure in the stack decreases along the cathode gas

Table 1
Coefficients and cell activation energy

	Magnitude	Unit
A_{ir}	9.84×10^{-3}	$\Omega\,cm^2$
ΔH_{ir}	23.8×10^{3}	J/mol
A_a	9.5×10^{-7}	$\Omega\,cm^2\,atm^{0.5}\,K^{-1}$
ΔH_a	27.9×10^{3}	J/mol
A_{c_1}	6.91×10^{-15}	$\Omega\,cm^2\,atm^{0.25}\,K^{-1}$
ΔH_{c_1}	179.2×10^{3}	J/mol
A_{c_2}	3.75×10^{-9}	$\Omega\,cm^2\,K^{-1}$
ΔH_{c_2}	67.2×10^{3}	J/mol
A_{c_3}	1.07×10^{-6}	–
ΔH_{c_3}	95.2×10^{3}	J/mol

Table 2
Regulating conditions for stable generation of MCFC stack

Location	Set condition	Purpose of the condition
An/Ca gas inlet	>600 °C	To prevent dissolution of NiO cathode
An/Ca gas outlet	<660 °C	To prevent corrosion of components
H_2 + CO utilisation	<85%	To avoid fuel mal-distribution in cell plane
Cathode pressure loss	<3 kPa	To prevent gas leakage
Cell voltage	>700 mV	Stability of the anode

Table 3
Calculation conditions for mass and heat balance in MCFC/GT system

Term	Value
Fuel composition	CH_4 (100%)
Reactive area of cell	1 m^2
Number of cells	200
Number of stacks	1
Performance of MCFC	Li/Na + press stamping
Air compressor adiabatic (isentropic) efficiency	75%
Expander adiabatic (isentropic) efficiency	80%
Cathode blower adiabatic (isentropic) efficiency	60%
Anode blower adiabatic (isentropic) efficiency	55%
Heat loss of fuel pre-heater	20% of heat flow
Heat loss of reformer	10% of combustion energy
Reforming temperature	750 °C
Reformer combustion temperature	800 °C
Electrical loss of total plant	2% of fuel energy
Inverter efficiency	95%
Electric motor efficiency	85%
Electric generator efficiency	85%

channel, therefore, the pressure loss in the cathode gas equals the pressure difference between cathode gas and pressure vessel. During the operation of the MCFC/GT system, the temperature of the stack is strongly related to the cathode gas flow rate and the inlet/outlet cathode gas temperature. Since the cathode gas is sealed by the wet-ability of the carbonate melt (liquid state), the pressure difference between cathode gas and pressure vessel should be less than 3 kPa to avoid a gas leakage. All of the values listed in Table 2 are taken into account in the material and heat balance calculation procedure in this paper; other conditions of the calculation procedure are listed in Table 3.

2.4. Relation between CH_4 reforming ratio and fuel utilisation

The main issue of this paper is the relation between the MCFC system performance and the operating pressure. According to the CH_4 reforming reaction of Eq. (1), the total mole number increases when H_2 and CO are produced; thus the CH_4 reforming ratio decreases by increasing the operating pressure. Once the CH_4 reforming ratio diminishes, the H_2 and CO flow rate in the anode gas channel decreases. H_2 + CO utilisation and CH_4 utilisation are defined in Eqs. (11) and (12), respectively. As determined in Table 2, the H_2 + CO utilisation should be kept lower than 85% to avoid a mal-distribution of fuel gas in the anode gas channel before the anode oxidation occurs; the additional natural gas supply is required under high-pressure operating conditions (CH_4 utilisation should be decreased)

$$CH_4\ \text{utilisation} = \frac{\text{fuel consumption rate due to anode reaction of Eq. (3)}}{4CH_4\ \text{flow rate at reformer inlet}} \tag{11}$$

$$(H_2 + CO)\ \text{utilisation} = \frac{\text{fuel consumption rate due to anode reaction of Eq. (3)}}{H_2 + CO\ \text{flow rate at anode inlet}} \tag{12}$$

In Fig. 2, the CH_4 utilisation and the H_2 + CO utilisation is plotted versus the system's operating pressure. The CH_4 reforming ratio is also related to the operating pressure in the axis on the right-hand side of Fig. 2, with a steam/carbon ratio of 3.25. The CH_4 utilisation is set at 80% when the operating pressure is 0.3 MPa, however, the CH_4 utilisation

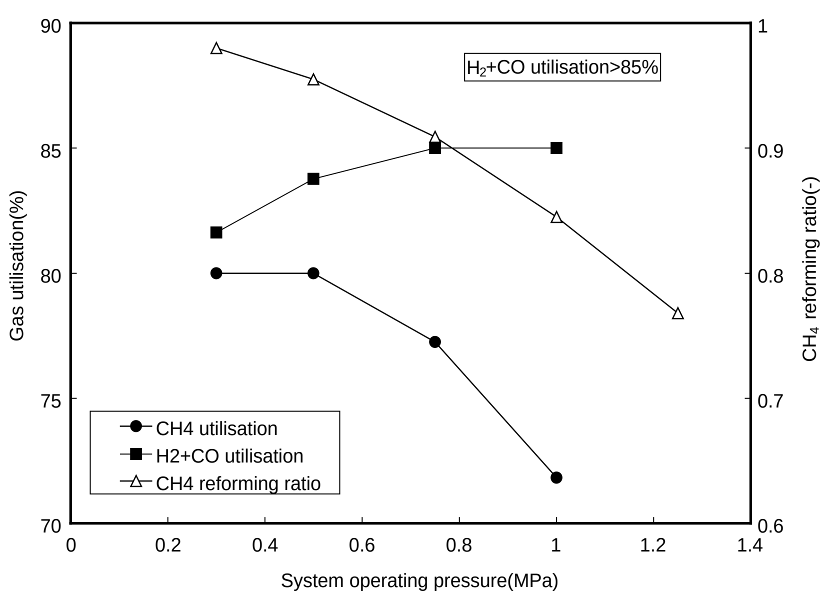

Fig. 2. Ch_4 and H_2 + CO utilisation with CH_4 reforming ratio vs. system operating pressure.

Table 4
Characteristics of analysed system and air flow rates

System case	Characteristic of the system	Air flow rate	Cooling of cathode re-circulating gas
1	Pressure ratio: 0.75 MPa (constant), air flow rate: constant	Adequate at 3000 A/m^2	No
2	Same as case 1	Adequate at 1500 A/m^2	Works at more than 1500 A/m^2
3	Pressure ratio: variable, air flow rate: function of pressure ratio	Adequate at 0.3 MPa, 1500 A/m^2	Same as case 2
4	Case 3 + anode recycling + sub-reformer	Same as case 3	Same as case 2

should be decreased at an operating pressure of approx. 0.75 MPa to keep the H_2 + CO utilisation at less than 85%. As expressed in the latter section of case 4, the anode recycling equipment with sub-reformer works at an operating pressure of more than 0.75 MPa to keep the H_2 + CO utilisation below 85%.

ating conditions. In the discussed four systems, the combustor in the GT cycle is eliminated to achieve a better thermal efficiency in partial load conditions. Thus, in order to simplify the system control, the air compressor and the expander were divided; the other specifications, which do not appear in Table 3, were never changed during the calculation period. The thermal efficiency is defined as follows:

$$\text{thermal efficiency} = \frac{\begin{array}{l}[\text{MCFC ac output}] + [\text{expander output}] - [\text{air compressor consumption}] \\ \quad - [\text{cathode blower consumption}] - [\text{anode blower consumption (case 4 only)}] \\ \quad - [\text{feed water pump consumption}]\end{array}}{\begin{array}{l}[\text{calorific value of } CH_4] \\ \quad - \text{other consumption (2\% of supplied } CH_4 \text{ calorific value)}\end{array}} \quad (13)$$

3. Results

The features and configurations of the four systems compared are presented in Table 4 and Fig. 3, respectively. The material and heat balance calculation results of the air compressor and the expander (GT cycle) are the same in both, the reference system and the four systems compared (Figs. 1 and 3); however, a combustion of fuel gas in the GT cycle obstructed the good thermal efficiency in partial load operating conditions.

3.1. System performance of basic system (case 1)

The basic system is the simplest system, designed for a current density of 3000 A/m^2 and an operating pressure of 0.75 MPa; the airflow rate is sufficient to keep the stack temperature at 600–660 °C. The cell voltage is more than 700 mV, which is high enough for a stable operation of the stack (cell voltage not shown). In Fig. 4, the thermal efficiency is expressed in relation to the electrical output of the system. If the current density is decreased during par-

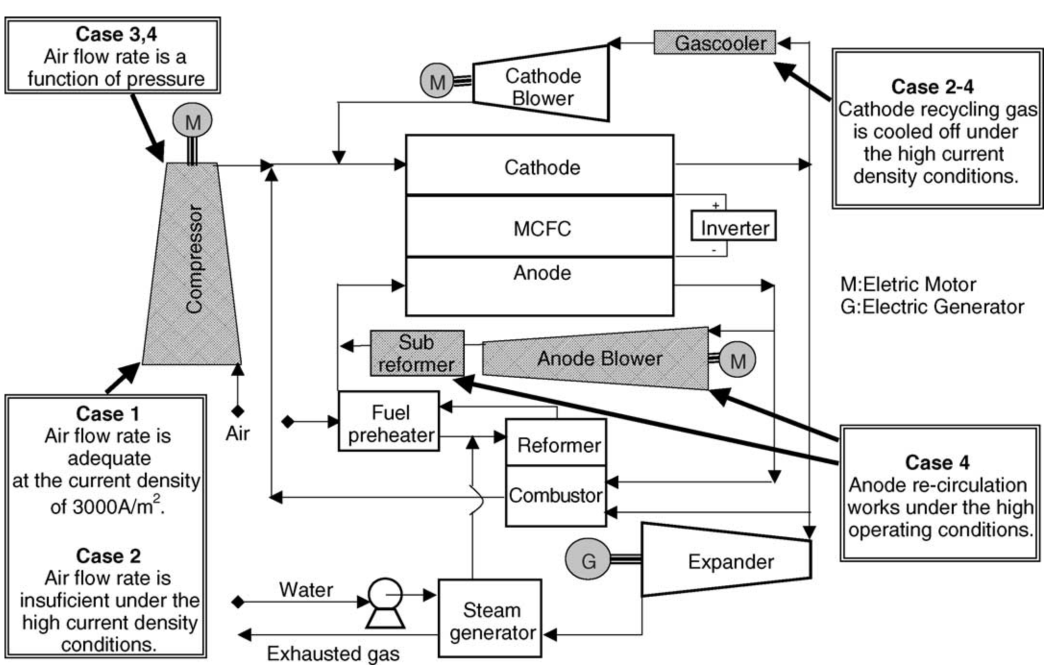

Fig. 3. Configurations of four system cases.

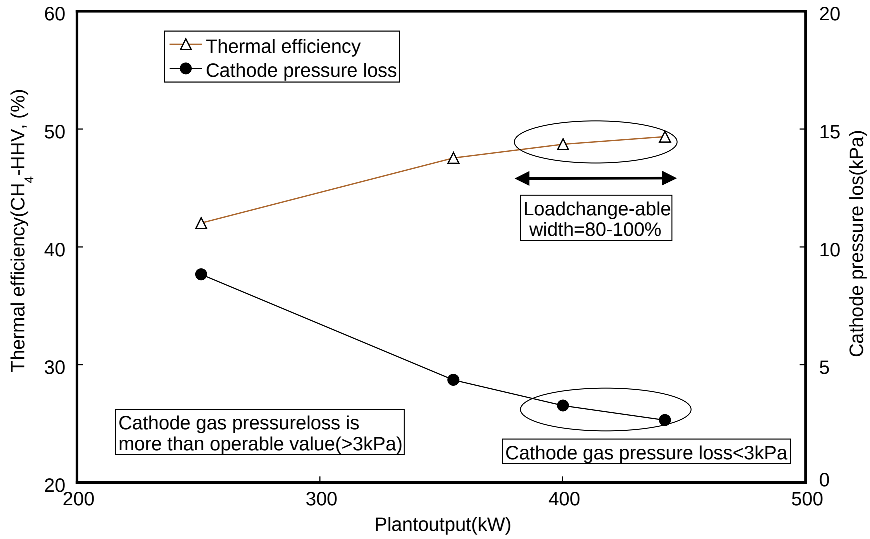

Fig. 4. Thermal efficiency and cathode pressure loss at partial load in system case 1.

tial load operation, the outlet gas temperature of the MCFC stack also decreases. To keep the cathode inlet gas temperature at 600 °C, a greater amount of cathode outlet gas needs to be recycled to the cathode inlet. This increase of cathode recycling gas leads to an increase of the cathode gas flow rate within the stack, which then also increases the pressure loss of the cathode gas. In Fig. 4, the pressure loss of the cathode gas and the power output of the plant are related to the partial load operation of the system. If the current density is set at less than 2500 A/m^2 (current density not shown), the pressure loss of the cathode gas is more than 3 kPa. According to these calculated results, case 1 can only be operated with an electrical power output of 80–100%.

3.2. *Combination of low flow rate air compressor and cooling of cathode recycling gas (case 2)*

In order to avoid a flood of cathode gas like in case 1, a small flow rate air-compressor is applied in case 2. If this system is operated under high current density conditions, the stack temperature rises above 660 °C. Therefore the system is equipped with a gas cooler in the cathode gas recycling line, which works at an operating current density of more than 1500 A/m^2.

In Fig. 5, the calculated cell voltage and the O_2/CO_2 ratio in the cathode inlet gas are presented versus the current density. The cell voltage remains at more than 700 mV at an operating current density of 3000 A/m^2. The change

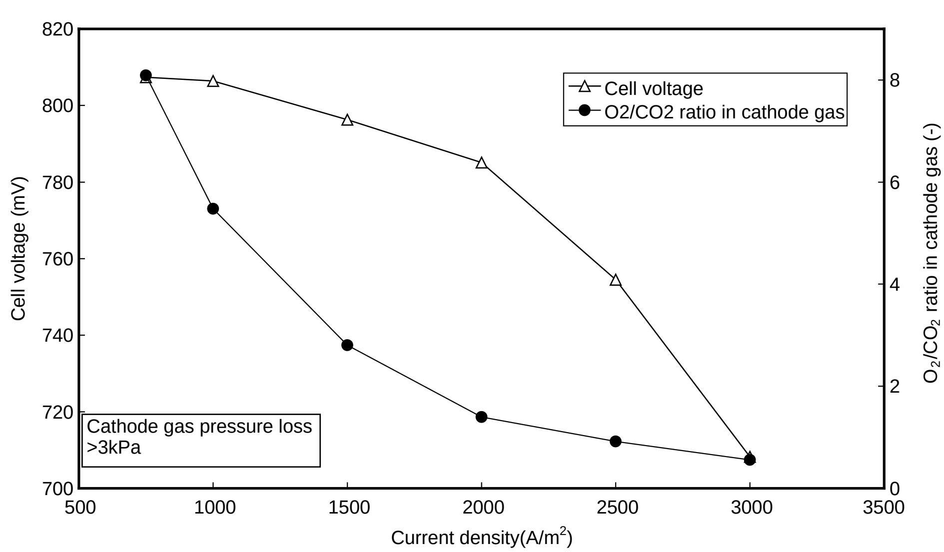

Fig. 5. Cell voltage and O_2/CO_2 ratio of cathode inlet gas vs. operating current density in system case 2.

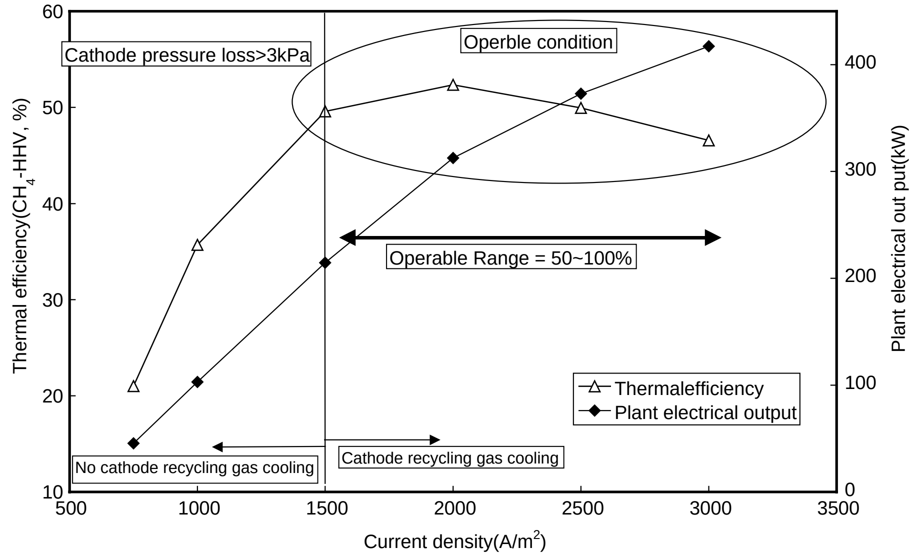

Fig. 6. Thermal efficiency and electrical plant output at partial load operation in system case 2.

of the cell voltage due to increasing the current density is small in this case (only 100 mV change between 750 and 3000 A/m^2). This is because the cell voltage drop due to internal resistance is small but the cathode polarisation is high (O_2/CO_2 ratio is high) under low current density conditions; the cell voltage drop due to internal resistance is large but the cathode polarisation is small (O_2/CO_2 ratio close to equivalent value of 0.5) under high current density conditions.

In Fig. 6, the calculated thermal efficiency and the power output are plotted versus the current density. If the system is operated at a current density lower than approx. 1250 A/m^2, the pressure loss of the cathode gas exceeds 3 kPa for the same reason as in case 1 (cathode pressure loss not displayed). The maximum thermal efficiency is determined at an operating current density of approx. 2000 A/m^2. The operable load range of case 2 is 50–100%, which is an improvement in comparison to case 1.

3.3. Pressure swing air compressor and cooling of cathode recycling gas (case 3)

In order to enlarge the operable load range of case 2, the minimum operable load needs to be expanded. Since the lowest load ratio is regulated by the cathode pressure loss, 3 kPa, in case 1 and 2, decreasing the airflow rate during partial load operation seems to be an effective measure. In case 3, a pressure swing air compressor is applied; the airflow rate of the air compressor changes according to the compressor's pressure ratio as shown in Fig. 7.

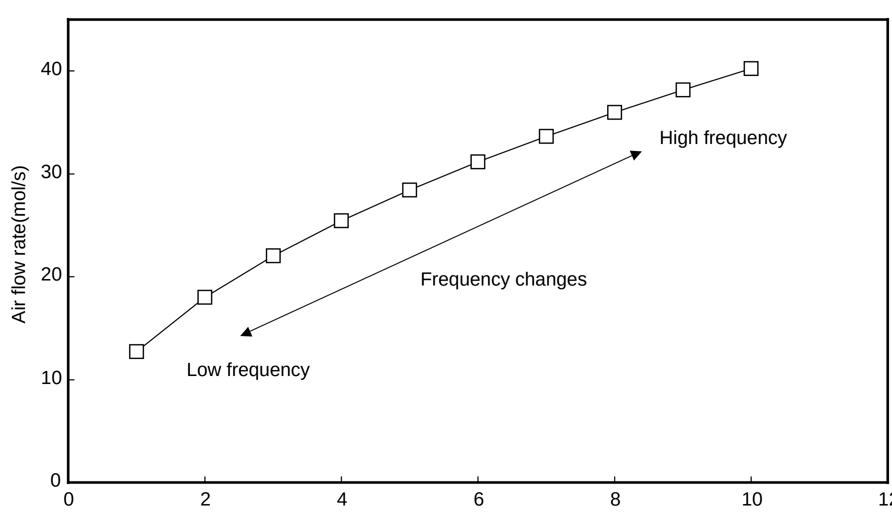

Fig. 7. Relation between airflow rate and pressure ratio with frequency parameter (frequency not shown).

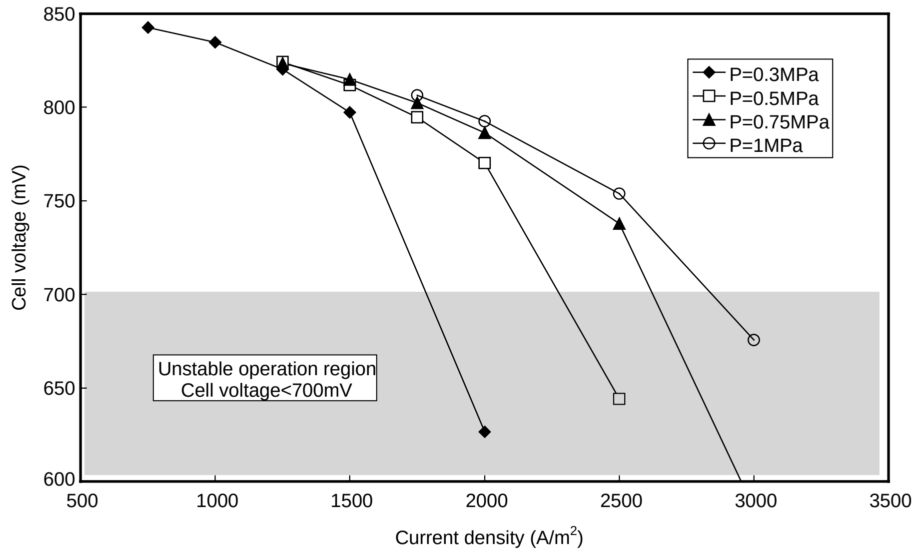

Fig. 8. Cell voltage vs. operating current density with operating pressure parameters (case 3).

In Figs. 8 and 9, the calculated cell voltage and the thermal efficiency are plotted in relation to the current density, respectively. Under low operating pressure conditions, for instance 0.3 MPa, the airflow rate is small; the cell voltage, when operated at high current density, 2000 A/m^2, decreases to less than 700 mV. In high operating pressure conditions (e.g. 1 MPa), the air supply rate is sufficient to maintain a stable cell voltage around 2750 A/m^2. The maximum efficiency in case 3 is determined at an operating pressure of approx. 0.5–0.75 MPa. The efficiency at an operating pressure of 1 MPa is low due to the decrease of the CH_4 reforming ratio at high operating pressure, because the fuel gas condition is limited by a maximum H_2 + CO utilisation of 85%. Case 3 can be operated at a current density of 750–2750 A/m^2, however, the thermal efficiency under high current density is lower than that at partial load.

3.4. Anode recycling with sub-reformer under high operating pressure (case 4)

In order to improve the thermal efficiency under high current density (high pressure) conditions of case 3, an anode recycling blower with a sub-reformer is added to the system case 4. The sub-reformer is a simple design of the adiabatic reformer [9]. The anode blower works at operating pressures more than 0.75 MPa to keep the H_2 + CO utilisation in the anode gas channel lower than 85%.

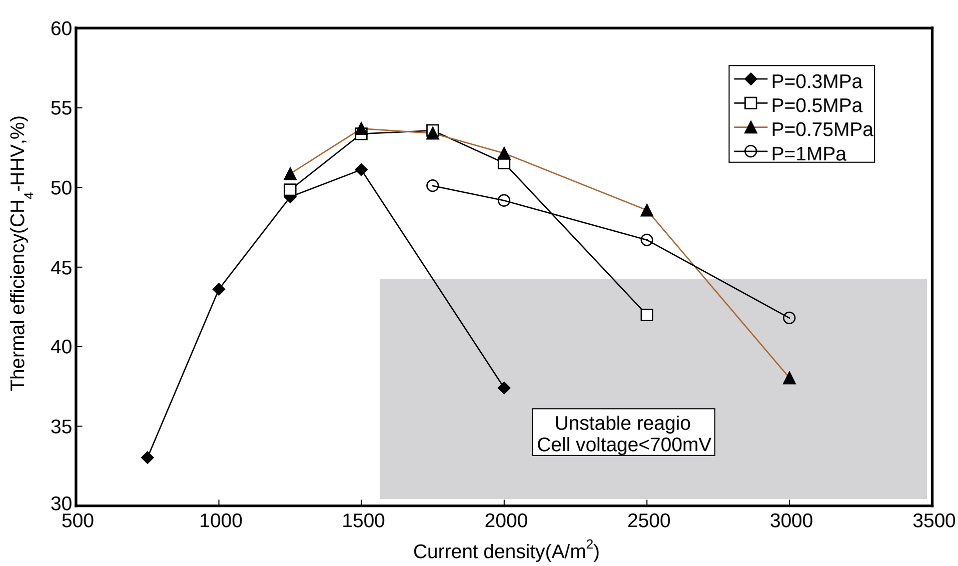

Fig. 9. Thermal efficiency vs. operating current density with operating pressure parameters in system case 3.

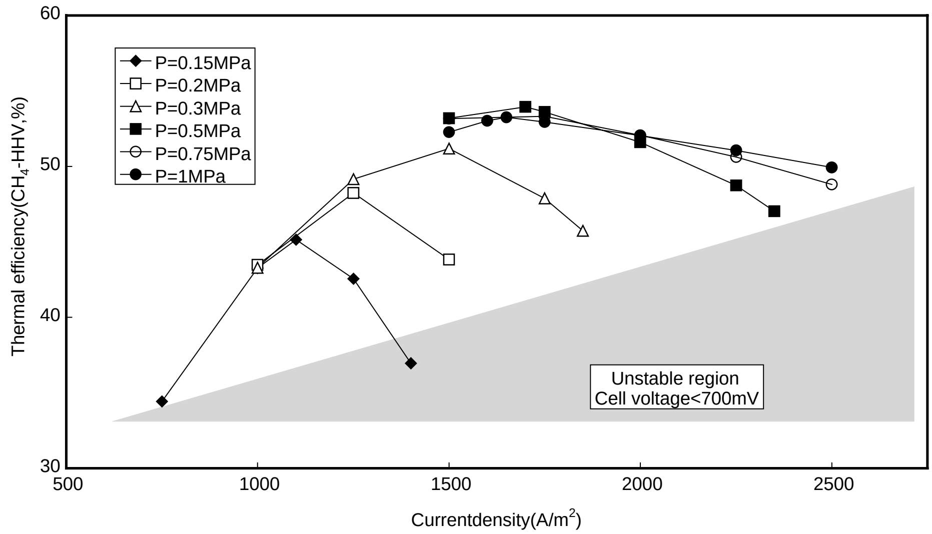

Fig. 10. Thermal efficiency vs. operating current density in system case 4.

In Fig. 10, the thermal efficiency of case 4 is related to the current density with the parameters of the operating pressure. When the current density is set at 2500 A/m^2, the thermal efficiency at an operating pressure of 1 MPa is higher, 50% HHV-CH_4, than the operating pressure of 0.75 MPa. This increase of thermal efficiency at high current density originates from the additional fuel reforming of the exhausted anode gas in the sub-reformer.

4. Discussions

In Fig. 11, the thermal efficiency of the four systems and the reference system is compared versus the system load rate. The maximum thermal efficiency of the reference system is around 54% at a load ratio of 100%, which is the optimised combination of the MCFC capacity and the gas turbine. In case 3, the thermal efficiency at partial load is improved compared to the reference system, however, the efficiency at a 100% load is lower than that in the reference system; the load ratio of case 3 can be changed from 30% to 100%. In case 4, the efficiency at a 100% load is better than case 3, and the minimum operable load can be set at around 20%. The operable range of cases 1 and 2 are limited mainly by the pressure loss in the cathode gas, whereas the operable range is enlarged by the pressure swing operation in system cases 3 and 4. The maximum thermal efficiency of system cases 3 and 4 is obtained at middle load range, thus the system has an advantage over the load changeable power generation systems.

An additional advantage of the pressure swing operation (system cases 3 and 4) is the low CO_2 partial pressure in partial load operation. The CO_2 partial pressure of the cathode gas is low because the operating pressure of the MCFC

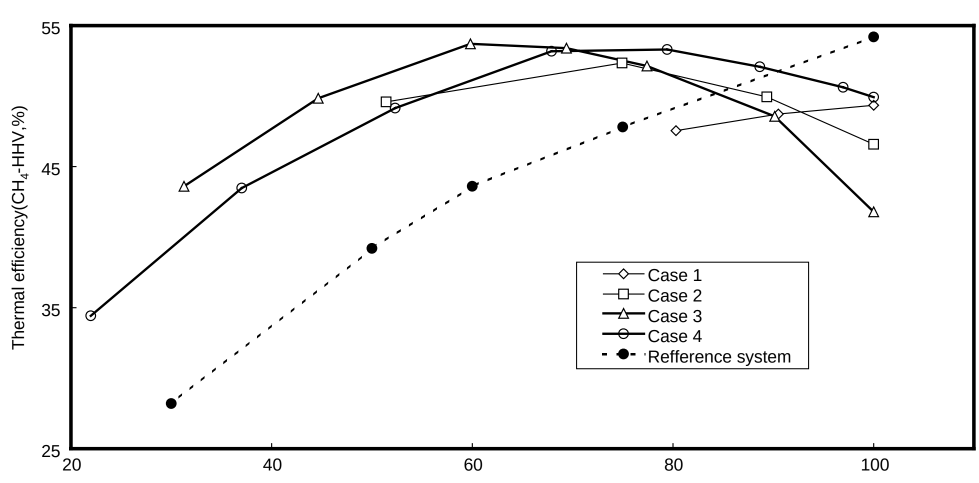

Fig. 11. Comparison of thermal efficiency in partial load condition with a reference system.

stack has decreased (CO_2 partial pressure not displayed); lower CO_2 partial pressure of the cathode gas is preferable for a longer Ni shortening time.

5. Conclusion

The material and the heat balance in partial load operating conditions of MCFC systems have been examined in the four systems. A constant pressure air compressor is applied in system cases 1 and 2, whereas a pressure swing air compressor is equipped in system cases 3 and 4. There is a cathode recycling gas cooler in cases 2–4, and an anode recycling line with additional reformer is provided in case 4; the thermal efficiency of each system case is compared versus the system load ratio. In the calculation procedure, the maximum cathode gas pressure loss is kept below 3 kPa. The following can be concluded:

(1) The range of the power load is limited to 50–100% in the constant operating pressure system, mainly because of the limited cathode gas pressure loss (cases 1 and 2).
(2) By applying a pressure swing air compressor (variable rotation air-compressor) with a gas cooler in the cathode recycling gas, the range of the power load is enlarged to 20–100% (cases 3 and 4).

According to these comparisons of thermal efficiency in partial load operating conditions, a combination of pressure swing air compressor (variable rotation air-compressor) and gas cooling in the cathode recycling line lead to a wider range of operations with high thermal efficiency.

References

[1] Y. Mugikura, K. Asano, Elect. Eng. Jpn. 138 (1) (2002).
[2] A.F. Massardo, B. Bosio, J. Eng. Gas Turbines Power ASME 124 (2002) 103–109.
[3] A.F. Massardo, F. Lubelli, J. Eng. Gas Turbines Power ASME 122 (2002) 27–35.
[4] H. Uechi, S. Kimijima, N. Kasagi, JSME B 68 (666) (2002) 336–345.
[5] J. Palsson, A. Selimovic, L. Sjunnesson, in: Proceedings of the Third IFCC, Japan, November 1999, pp. 391–394.
[6] S. Campanari, J. Eng. Gas Turbines Power ASME 122 (2000) 239–246.
[7] P. Costamagna, L. Magistri, A.F. Massardo, J. Power Sour. 96 (2001) 352–368.
[8] S. Kimijima, N. Kasagi, in: Proceedings of the ASME TURBO EXPO 2002, 3–6 June 2002, Amsterdam, The Netherlands.
[9] H. Yasue, in: Proceedings of the Third IFCC, Japan, 1999, pp. 251–255.
[10] K. Itou, in: Proceedings of the Third IFCC, Japan, 1999, pp. 313–316.
[11] H. Morita, J. Power Sour. 112 (2002) 509–518.